

Stratigraphic Correlation via Opportunity's Pancam of the Burns Formation, Meridiani Planum, Mars. S. D. Thompson¹, W. M. Calvin¹, and the Athena Science Team, ¹Dept. of Geological Sciences MS-172, University of Nevada, Reno, Reno NV 89557-0180 (thomp102@unr.nevada.edu).

Introduction: For over three Earth years the Mars Exploration Rover, Opportunity, has investigated, via remote sensing and *in situ* observations, an extensive occurrence of hematite and sulfate-salt rich sedimentary bedrock exposures in crater walls and plains surfaces [1]. These observations have occurred over ~10 kilometers of traverse odometry from the landing site to Victoria crater (Figure 1). The sedimentary bedrock has been named the Burns formation in honor of Roger Burns, who predicted sulfate deposits on Mars, particularly in the form of jarosite. Farrand *et al.* [2] have described the major spectral properties of the Burns formation in the craters Eagle and Endurance as observed by Pancam. Grotzinger *et al.* [3] and McLennan *et al.* [4] have described the stratigraphic record based on primary and secondary structures. This analysis looks at Pancam multispectral data acquired during Opportunity's mission from landing to sol 1037. We analyzed nearby (<~10 m) rock targets with Pancam where sufficient spatial resolution (<10 mm) is achieved to obtain spectral parameters of individual sedimentary structures as well as erosional and possible secondary diagenetic features (i.e., fracture fill and rind materials). Supplemental data in the analyses include Microscopic Imager (MI) images along with Mössbauer spectrometer and Alpha Particle X-ray Spectrometer (APXS) data. Finally, the classification of the Burns formation from the above instruments (primarily Pancam) are discussed in relation to the multiple data sets available for Meridiani Planum acquired from orbit and to the pending hypotheses.

Geologic Setting: The outcrop materials of the Burns formation observed by Opportunity are close to the top of near horizontal sedimentary stack of layered deposits totaling ~800 m in thickness [5] and overlying Late Noachian aged cratered terrains within the Meridiani Planum region. Investigation of these sediments, at least locally, has shown sub-centimeter thinly laminated deposits with few occurrences of festoon cross-bedding, massive bedding [3], and subtle differences in color [2].

Regional observations show the Burns formation extending hundreds of kilometers maintaining uniformity with margin outliers of buttes, mesas, and yardangs-like features indicating a more extensive unit when emplaced [6]. Hynek *et al.* [6] and Arvidson *et al.* [7] concluded that the layered

deposits are volcanic air fall ash layers even though no recognizable construct is visible in the region.

The site occurrence of the Meridiani Planum sediments being basaltic-andesitic in composition with ~10-15% hematite are consistent with a volcanic origin, however there are no sizeable volcanic constructs in the region [8]. It is possible that the

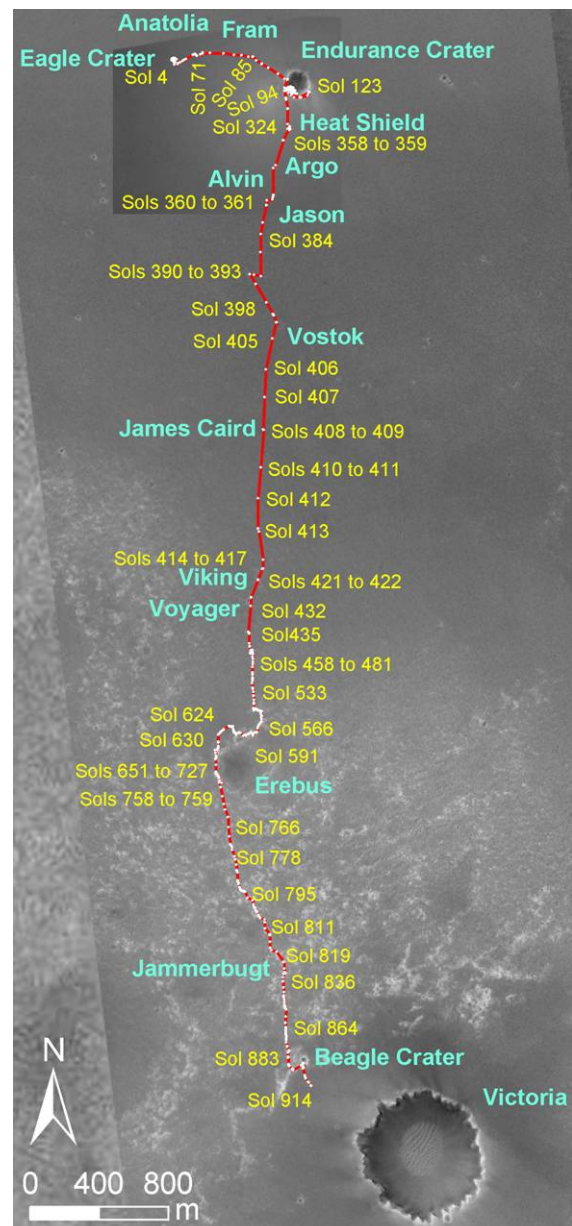


Figure 1. Traverse map of the excursion performed by Opportunity. Blue labels are names of significant features along traverse. (OSU Mapping and GIS laboratory)

locale is underlain by ancient volcanic flows and the layered deposits are volcanoclastic materials. Fe-rich ash could have been laid down and then later oxidized to hematite through fluid flow. Also, the volcanic source may be currently buried by the sediments. If the materials are air fall deposits, they could have come from 1000s of kilometers away. However, if the deposits did come from this distance, there should be more hematite occurrences than have been observed. They could be buried, removed by erosion, or have hematite concentrations below the detection limit of TES.

A regional water table in the area during one or more portions of the Hesperian could be responsible for the formation of hematite as a secondary diagenetic process. It is suggested that the layered deposits were in place before the regional flooding and may have interacted with Early Hesperian aquifers in the area. The uniqueness of hematite occurring on Mars, in general, may be a result of a timely interaction of magmatic heating, groundwater circulation, and catastrophic release of water. Differential erosion of the layered sediments in the form of resistant ridges, buttes and mesas, may represent the cementation along joints and weak bedding planes from groundwater flow.

Opportunity explored ~7 m of stratigraphic section in the walls of Eagle, Fram, Endurance (Figure 2), and Victoria craters and various exposures within the hematite-basaltic sand-rich surface veneer. The rover has found that the light-toned sedimentary rocks are cross-bedded siliciclastic sandstones altered by diagenesis in the presence of sulfur-rich, acidic groundwater [1,4]. Sand grains range from 0.3 to 0.8 mm in size and vary from lamina to lamina but seem to have a bimodal sorting that generally includes the larger grains into one layer, and finer ones into others [3].

OMEGA data from Mars Express is interpreted to indicate the presence of absorbed molecular water and sulfate minerals with some differences in the layered units [9]. Many sulfate minerals are present jarosite and Ca- and Mg-sulfates despite local changes in elemental abundances [10].

Methodology: Pancam multispectral data are acquired with 11 channels from 443 to 1009 nm (visible/near infrared, or VNIR) with bandwidths ranging from 16 to 28 nm providing calibrated I/F data (where I is the measured scene radiance and πF is the solar irradiance at the top of the martian atmosphere) which is divided by the cosine of the solar incidence angle to produce the quantity R^* [11]. All complete multispectral data sets of targeted observations were analyzed for exposed bedrock features within 10m. This subset of data was then examined for spectral differences in the laminar sedimentary structures (i.e., Figure 3a) both locally and to a lateral extent. After making spectral classifications and spatial statistical analyses of the bedrock materials, the locations are then correlated to the morphologic and mineralogic descriptions that have been observed.

Common spectral parameters calculated through image processing for analysis include those shown in Table 1. Other image products generated from the calibrated data were decorrelation stretch (DCS) images (i.e., Figure 3b). DCS images are 3-color composites of image products from principle components analysis used to help dramatically increase subtle color contrasts within the scene [12] and provide context for locating unique spectral signatures. 10 to 50 pixels of single continuous rock layers were selected within the multispectral data cubes for spectrum plots to characterize fine scale color differences.

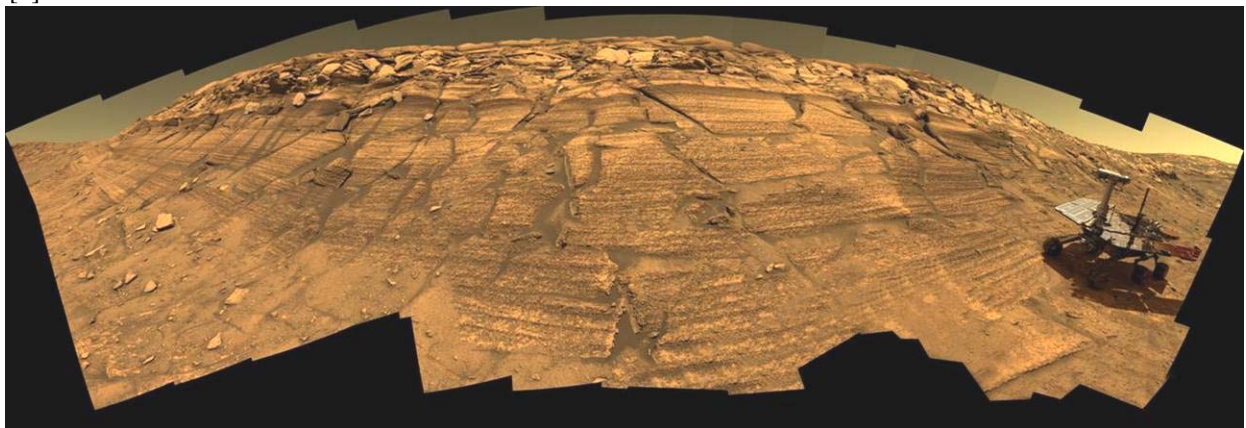


Figure 2. Pancam mosaic of the Burns fm with all ~7 m of stratigraphy exposed within Endurance crater. The lowermost unit is only well exposed below the disconformable contact to the far left.

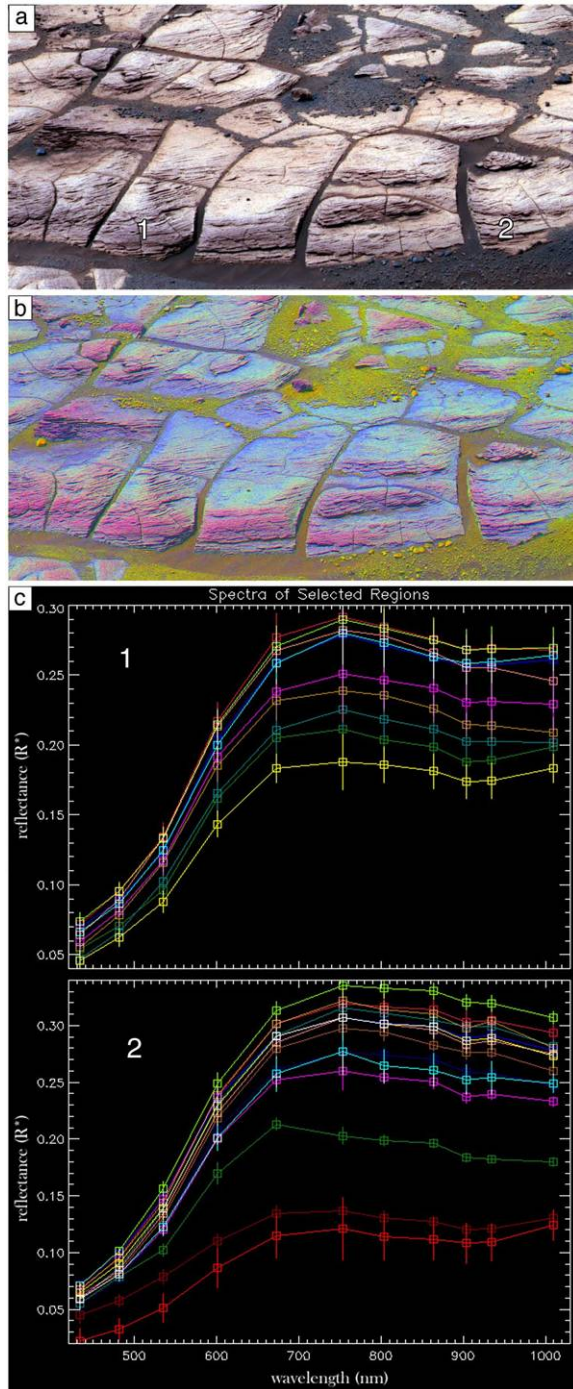


Figure 3. Example outcrop material in a color (601, 535, and 482 nm) composite (a) and a DCS image (b) from the 432, 535, and 753 nm bands from sol 648 Pancam sequence P2574. The spectral plots (c) are from individual layers of the rock fragments 1 and 2 as annotated in (a). The dark green spectrum from rock 2 is a layer like the rest based on color but has a slope sign change from 673 to 753 nm unlike the other plots. The two red shallow profiles in c-2 are of soil and rind materials near the base of the rock. Error bars represent standard deviations of pixels in selected regions of interest.

Results: Analysis of the spectral parameters from selected regions included individual laminations of bedding, exposed bedrock topographic surfaces from horizontal to vertical orientations, variations in color and/or texture, loose fragmented materials on the surface layer, poorly- and well-sorted basaltic sand material, and the hematite-rich spherules. Shadowed areas typically have similar signatures as the adjacent sunlit areas with much lower reflectance values but can produce unusual behaviors. Therefore, strong shadowed areas are not considered. Another spectral influence could be photometric effects, especially at extreme solar incidence angles [13].

Most bedrock spectra exhibit a steep positive slope in the visible region but subtle changes in the near infrared region. These changes include broad variances from flat to concave to convex in the 753 nm to 1009 nm region and narrow features in the 904 or 934 nm bands. Maxima are typically in the 750-850 nm region but can occur as low as the 673 nm band and as high as the 1009 nm band with the latter usually from the lowest albedo materials (i.e., spherules and basaltic sands).

Figure 3c shows spectra of individual bedrock layers of two rocks (labeled 1 and 2) from Figure 3a. A major difference between them is in the slope of the 934 and 1009 nm bands where rock 1 has several occurrences of a positive slope whereas rock 2 has stronger negative slopes from 934 to 1009 nm. Positive slopes are consistent with the presence of hematite possibly associated with the spherules [2].

Band depth images centered at 535 and 904 nm provide statistics on the relative occurrences of crystalline ferric oxide minerals. Ferric iron-bearing phases also strongly affect the 600 nm region. The hematite spherules have the largest 904 nm band depths. The dark green spectrum in Figure 3c, rock 2, is from one particular layer with a slightly stronger 535 nm band absorption. More common is the 904 nm feature, which is understood as an artifact in the image data calibration but strong absorptions with small error here are considered to be real color differences.

Common occurrences of iron-rich signatures appear in materials close to the soil surface and on more vertical surfaces. The highest albedo rock surfaces also tend to have the strongest negative slope in the longer wavelengths. This could be a result of an intrinsic characteristic of the outcrop material or perhaps a significantly thick (e.g. >100 micron) dust deposit [13].

Rarely, iron-rich signatures are present in one lamination and not in the surrounding layers, although such an occurrence could result from a

single iron-rich primary sedimentary episode, a secondary diagenetic product of cementation concentration, or associated with a vein or fracture fill material. However, this may also be an artifact of photometry or dust layer thickness differences.

Material overlying the bedrock is substantially basaltic sand with contributions of hematite spherule and fragmented spherule material [14]. The spherules and sand spectra both have strong hematite signatures. Pancam can be used to compare VNIR signatures of remotely sensed near-field and far-field scenes with those analyzed in more detail with the other Athena payload instruments, Mössbauer, Alpha Particle X-ray and Mini-TES spectrometers as well as data acquired from spaceborne platforms (i.e., Mars Global Surveyor, Mars Odyssey, Mars Express, Mars Reconnaissance Orbiter).

Spatial statistics were done using Correspondence Analysis techniques based on selected spectral profiles to search for similarities and/or differences in color along the traverse as shown in figure 1. Figure 4 shows the plot of spectra averages from 23 different sites selected in rough equal distances along the traverse. For the most part, few differences exist, however there are a few locations that do correlate or not correlate strongly with one another. Sites observed on sols 27 and 553 (ID nos. 1 and 13) correlate very strongly and are unique from the other sites based on separation from the clustered data in the upper right of figure 4. Spectra from the scene on sol 38 (ID no. 2) does not correlate with any of the other analyzed samples.

Pancam spectra obtained for materials investigated with the *in situ* instruments can act as “ground truth” spectra for comparison with the “Pancam only” observed targets and the rover data can be extrapolated data from the orbiters. This provides an extensive and highly detailed data set to correlate both laterally and stratigraphically, of the exposed bedrock materials of Meridiani not just along the traverse accomplished by Opportunity, but also with orbital multispectral measurements of this and other regions on Mars.

Acknowledgements: Thanks to all the MER engineering and science teams for continued operations and effort to make this mission a success beyond expectations and to the Pancam team.

References: [1] Squyres, S.W. and A.H. Knoll (2005) EPSL, 240, 1-10. [2] Farrand W.H. *et al.*, (2006) JGR, 111, E02, S15. [3] Grotzinger, J.P. *et al.*, (2005) EPSL, 240, 11-72. [4] McLennan, S.M. *et al.*, (2005) EPSL 240, 95-121. [5] Edgett, K.S., (2005) Mars 1, 5-58. [6] Hynek, B.M. *et al.*, (2002) JGR, 107, E10, 5088. [7] Arvidson, R.E. *et al.*,

(2003) JGR, 108, E12, 8073. [8] Christensen, P.R. *et al.*, (2000) JGR, 105, E4, 9623. [9] Arvidson, R.E. *et al.*, (2005) SCIENCE, 307, 1591-1594. [10] Clark, B.C. *et al.*, (2005) EPSL, 240, 73-94. [11] Bell, J.F. *et al.*, (2003) JGR, 108, E12, 8063. [12] Gillespie, A.R. *et al.*, (1986) Remote Sens Environ, 20, 209-235. [13] Johnson, J.R. *et al.*, (2006) JGR Spirit issue, 111, E02, S14. [14] Soderblom, L.A. (2004) SCIENCE, 306, 1723-1726.

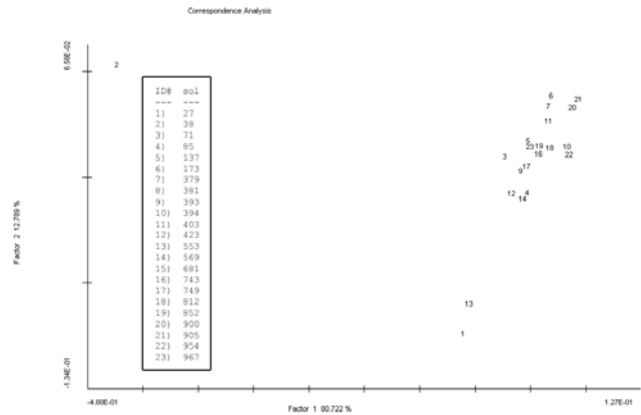


Figure 4. Spatial statistics plot using Correspondence Analysis technique to correlate selected spectra averages of 23 scenes equally distributed along the traverse from Eagle to Victoria craters. The inset table identifies the plot identifier with respect to which sol the data came from. The x-axis represents correlations with the highest confidence and the y-axis represents correlations with the second highest confidence. The closer these identifiers plot, the more correlative the data are.

Table 1. Spectral parameter descriptions.

Parameter	Description	Sensitivity
Red/Blue ratio	(753 nm / 432 nm)	Overall Albedo and color variations
1009 nm / 934 nm ratio	(1009 nm / 934 nm)	Hematite (spherules)
535 nm band depth	$[(0.57 \times R_{432}^* + (0.43 \times R_{673}^*)) - R_{535}^*]$	Ferric minerals
904 nm band depth	$[(0.51 \times R_{800}^* + (0.43 \times R_{1009}^*)) - R_{903}^*]$	Ferric minerals
934 to 1009 nm slope	$(R_{1009}^* - R_{934}^*) / (1009 - 934)$	Hematite (spherules)